Magnetostriction of Heusler Ferromagnetic Alloy, Ni$_2$MnGa$_{0.88}$Cu$_{0.12}$, around Martensitic Transition Temperature

Takuo Sakon [1,*], Koki Morikawa [1], Yasuo Narumi [2], Masayuki Hagiwara [2], Takeshi Kanomata [3], Hiroyuki Nojiri [4] and Yoshiya Adachi [5]

[1] Mechanics and Robotics Course, Faculty of Advanced Science and Technology, Ryukoku University, Otsu 520-2194, Shiga, Japan

[2] Center for Advanced High Magnetic Fields, Graduated School of Science, Osaka University, Toyonaka 560-0043, Osaka, Japan; narumi@ahmf.sci.osaka-u.ac.jp (Y.N.); hagiwara@ahmf.sci.osaka-u.ac.jp (M.H.)

[3] Research Institute for Engineering and Technology, Tohoku Gakuin University, Tagajo 985-8537, Miyagi, Japan; c1924007@mail.tohoku-gakuin.ac.jp

[4] Institute for Materials Research, Tohoku University, Sendai 980-8577, Miyagi, Japan; hiroyuki.nojiri.e8@tohoku.ac.jp

[5] Graduate School of Science and Engineering, Yamagata University, Yonezawa 992-8510, Yamagata, Japan; adachy@yz.yamagata-u.ac.jp

* Correspondence: sakon@rins.ryukoku.ac.jp

Abstract: In this study, magnetostriction measurements were performed on the ferromagnetic Heusler alloy, Ni$_2$MnGa$_{0.88}$Cu$_{0.12}$, which is characterized by the occurrence of the martensitic phase and ferromagnetic transitions at the same temperature. In the austenite and martensite phases, the alloy crystallizes in the $L2_1$ and $D0_{22}$-like crystal structure, respectively. As the crystal structure changes at the martensitic transition temperature (T_M), a large magnetostriction due to the martensitic and ferromagnetic transitions induced by magnetic fields is expected to occur. First, magnetization (*M-H*) measurements are performed, and metamagnetic transitions are observed in the magnetic field of $\mu_0 H = 4$ T at 344 K. This result shows that the phase transition was induced by the magnetic field under a constant temperature. Forced magnetostriction measurements ($\Delta L/L$) are then performed under a constant temperature and atmospheric pressure ($P = 0.1$ MPa). Magnetostriction up to 1300 ppm is observed around T_M. The magnetization results and magnetostriction measurements showed the occurrence of the magnetic-field-induced strain from the paramagnetic austenite phase to the ferromagnetic martensite phase. As a reference sample, we measure the magnetostriction of the Ni$_2$MnGa-type (Ni$_{50}$Mn$_{30}$Ga$_{20}$) alloy, which causes the martensite phase transition at $T_M = 315$ K. The measurement of magnetostriction at room temperature (298 K) showed a magnetostriction of 3300 ppm. The magnetostriction of Ni$_2$MnGa$_{0.88}$Cu$_{0.12}$ is observed to be one-third that of Ni$_{50}$Mn$_{30}$Ga$_{20}$ but larger than that of Terfenol-D (800 ppm), which is renowned as the giant magnetostriction alloy.

Keywords: Heusler alloy; Ni$_2$MnGa; ferromagnetism; shape memory alloy; magnetostriction; martensite

1. Introduction

Ferromagnetic Ni$_2$MnGa-type Heusler alloys are known as highly functional materials in applications such as smart actuators and robotics, which utilizes the magnetic field-induced strain (MFIS) [1–30], and magnetic refrigeration, which utilizes the magnetocaloric effect [31–36].

In our previous study, we performed thermal expansion, permeability, and magnetization measurements on Ni$_2$MnGa$_{0.88}$Cu$_{0.12}$ [37], which is commonly characterized by the occurrence of martensitic and ferromagnetic transitions at the same temperature. Its permeability abruptly changes and shows a clear peak around the martensitic transition

temperature, T_M. The temperature dependence of the magnetization also shows a clear decrease around T_M. The value of T_M obtained through linear expansion was 337 K. Furthermore, T_M and T_R (reverse martensitic transition temperature from martensite phase to austenite phase) increase gradually with increasing magnetic fields.

T_M of the ferromagnetic Heusler alloy, $Ni_2MnGa_{0.88}Cu_{0.12}$, in the magnetic field is considered to shift according to the magnetic fields, and it is proportional to the difference between the magnetization of austenite and martensite phases. The shift of T_M was estimated as $dT_M/d(\mu_0H) = 1.3$ K/T. Khovailo et al. [38–40] discussed the correlation between the shifts of T_M of $Ni_{2+x}Mn_{1-x}Ga$ ($0 \leq x \leq 0.19$) using theoretical calculations. The experimental values of this shift corresponded well with the theoretical calculation results. In general, in a magnetic field, the Gibbs free energy is lowered by the Zeeman energy $-\Delta MB$, which enhances the motive force of the martensitic transition. Thus, T_M of $Ni_2MnGa_{0.88}Cu_{0.12}$ is considered to have shifted in accordance with the magnetic fields because high magnetic fields are favorable to the ferromagnetic martensitic phases.

The $dT_M/d(\mu_0H)$ of $Ni_2MnGa_{0.88}Cu_{0.12}$ is larger than that of other Ni_2MnGa-type Heusler alloys [18,38,40,41], indicating that the magnetic fields considerably affect the martensitic transition of $Ni_2MnGa_{0.88}Cu_{0.12}$ compared to that of other alloys.

Mendonça et al. investigated the magnetizations and magnetostrictions of off-stoichiometric Ni_2MnGa-type polycrystalline $Ni_2Mn_{0.7}Cu_{0.3}Ga_{0.84}Al_{0.16}$ alloy [19]. At a temperature slightly higher than T_M, a magnetostriction, $\Delta L/L$, caused by the magneto-structural transition demonstrating a significant deformation of 26,000 ppm (2.6%) with metamagnetic transition from the low-magnetic field austenite to the high-magnetic field martensite phase was observed. Martensitic and ferromagnetic transitions occur at the same temperature of $T_M = 293$ K; this property is similar to that of $Ni_2MnGa_{0.88}Cu_{0.12}$ [37]. The shift of T_M was estimated as $dT_M/d(\mu_0H) = 1$ K/T, which is of the same order as that of $Ni_2MnGa_{0.88}Cu_{0.12}$. The temperature dependence of the magnetization M-T curve of $Ni_2Mn_{0.7}Cu_{0.3}Ga_{0.84}Al_{0.16}$ indicated the presence of a metamagnetic-like large hysteresis at 298 K. This, in turn, indicates that at a constant temperature, re-entrant transitions occur between the paramagnetic austenite phase and ferromagnetic martensite phase. In this study, the M-T curve of $Ni_2MnGa_{0.88}Cu_{0.12}$ indicated the metamagnetic-like large hysteresis at 343 and 345 K, which are slightly higher than T_M. Moreover, the metamagnetic behavior suggests that $Ni_2MnGa_{0.88}Cu_{0.12}$ can generate a large magnetostriction around T_M.

In this study, we analyzed the magnetostriction of $Ni_2MnGa_{0.88}Cu_{0.12}$ and compared its characteristics with those of other MFIS alloys.

2. Materials and Methods

2.1. Materials

The polycrystalline $Ni_2MnGa_{0.88}Cu_{0.12}$ sample was grown by repeated arc melting of the constituent elements, namely 4N Ni, 4N Mn, 4N Cu, and 6N Ga, in an Ar atmosphere. All reaction products were packed in evacuated silica tubes at 1123 K for 72 h and then at 873 K for 24 h before being quenched into water [42,43]. The samples were characterized using X-ray powder diffraction measurements based on Cu-Kα radiation. At room temperature, the crystalline structure was a tetragonal $D0_{22}$-like martensite. In addition, the results of the X-ray diffraction indicated that the tetragonal phase with a $D0_{22}$-like crystal structure coexists with the monoclinic phase of the monoclinic *14M* structure (space group: $P2/m$) at room temperature. The lattice parameters of $D0_{22}$ are $a_{D022} = 0.38920$ nm and $c_{D022} = 0.65105$ nm. The details of the preparation and characterization of the sample can be found in references [42,43]. As a result of having observed a sample by an optical microscope at 298 K, there are some grains as large as 0.1 mm, which size was smaller than that of polycrystalline $Ni_2Mn_{0.7}Cu_{0.3}Ga_{0.84}Al_{0.16}$ alloy (grain size 0.5 mm) [19].

A Ni_2MnGa-type single-crystalline alloy was purchased from Adaptamat Co., Ltd. (Helsinki, Finland). The materials were analyzed using EDS (6010LA, JEOL Co., Ltd., Akishima, Japan) at the Faculty of Advanced Science and Technology, Ryukoku University. The materials included 29.79 at.% Mn, 50.03 at.% Ni, and 20.18 at.% Ga. Therefore, the

alloy was transcribed into $Ni_{50}Mn_{30}Ga_{20}$. An alloy with similar lattice constants and crystal structure as this sample has been presented in [5]. At room temperature, the crystal structure was a 7-layered *7M* martensite (which corresponds to the *14M* structure and P2/m space group) with lattice constants of a = 0.4219 nm, b = 0.5600 nm, and c = 2.0977 nm. At 324 K, the crystal structure was transformed into cubic-$L2_1$ austenite (space group Fm3 m) with a lattice constant of a = 0.5837 nm.

2.2. Methods for Experimental Measurements

Magnetization measurements were performed using the SQUID magnetometer (MPMS-XL7, Quantum Design Co., Ltd., San Diego, CA, USA) at the Center for Advanced High Magnetic Fields, Osaka University. The sample size of $Ni_2MnGa_{0.88}Cu_{0.12}$ for the magnetization measurement was $1.4 \times 1.4 \times 1.4$ mm. The magnetization process *M-H* measurements were performed at temperatures ranging from 360 K to 330 K. Each measurement point took 30 s. Temperature dependence of the magnetization *M-T* measurements were performed by warming the sample from 310 K to 400 K, followed by cooling from 400 K to 310 K. The temperature sweep ratio was 0.016 K/s. Each measurement point took 60 s.

Magnetostriction measurements were carried out using strain gauges KFR-02-120-C1-16 (Kyowa Dengyo Co., Ltd., Chofu, Japan) under atmospheric pressure and without applying any pre-stress. The base size of this strain gauge is 2.5 mm (parallel to the grid) $\times$ 2.2 mm. The electrical resistivity of the strain gauges was measured using the four-probe method and was measured by means of 2000/J digital voltmeter (Keithley Co., Ltd., Cleveland, OH, USA). This digital voltmeter was connected to a CF-FX1 Laptop PC (Panasonic Co., Ltd., Kadoma, Japan) via a GPIB cable, and measured by means of Basic 98 program. The sample size of $Ni_2MnGa_{0.88}Cu_{0.12}$ is $3.5 \times 3.0 \times 3.0$ mm. The magnetostrictions of $Ni_2MnGa_{0.88}Cu_{0.12}$ were measured parallel to the applied magnetic field ($\Delta L/L$)//H. The sweep speed of the magnetic field during the magnetostriction measurement was 0.0125 T/s. Each magnetostriction measurement at a specific temperature was measured after heating the sample to 370 K, which is higher than T_R, and then maintaining a constant temperature. In order to estimate the error of the strain gauge, the strain gauge was fixed on Cu plate, and the magnetoresistance of the strain gauge was measured in a magnetic field up to 10 T. The error was estimated to be ± 1 ppm at 5 T and ± 3 ppm at 10 T.

The forced magnetostriction measurements for $Ni_2MnGa_{0.88}Cu_{0.12}$ were performed using a helium-free superconducting magnet up to 6 T at the Center for Advanced High Magnetic Field Science, Osaka University, and up to 9.8 T at the High Field Laboratory for Superconducting Materials, Institute for Materials Research, Tohoku University.

The forced magnetostriction measurement for $Ni_{50}Mn_{30}Ga_{20}$ was performed using a four-prove strain gauge method up to 1.5 T with a water-cooled electromagnet (Tamagawa Seisakusho Co., Ltd., Sendai, Japan) at the Faculty of Advanced Science and Technology, Ryukoku University. The sample size was $3.5 \times 2.5 \times 1.0$ mm, and the longitudinal direction of the sample was parallel to the *c*-axis. The magnetostriction was measured along the *c*-axis in a magnetic field applied parallel to the *c*-axis, ($\Delta L/L$)//H//c.

3. Results and Discussions

3.1. Temperature and Magnetic Field Dependency of the Magnetization

Figure 1 shows the temperature dependence of the magnetization for $Ni_2MnGa_{0.88}Cu_{0.12}$ in a magnetic field of μ_0H = 0.1 T. The low- and high-temperature phases below and above 340 K indicate the ferromagnetic martensite and paramagnetic austenite phases, respectively. This is consistent with the results of previous studies [37,42,43]. The reason of the dip of the magnetization *M-T* curve around 325 K in cooling process, and the difference of the *M-T* curve in cooling and heating processes shown in Figure 1, can be attributed to the alignment of magnetic moments of Mn and Ni atoms parallel to the magnetic field just below T_M and the rearrangement of the *14M* and/or DO_{22} tetragonal lattices by the magnetic moments.
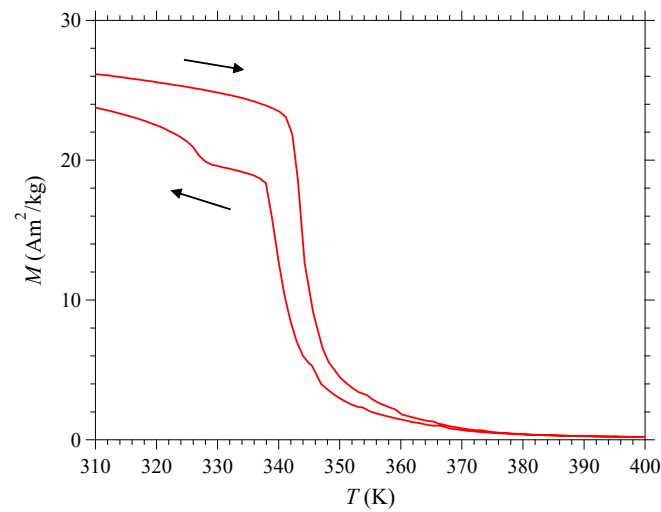
Figure 1. Temperature dependence of the magnetization, *M* vs. *T*, for $Ni_2MnGa_{0.88}Cu_{0.12}$ in a magnetic field of 0.1 T. The arrows show the process of the temperature.

The values of *dM/dT* shown in Figure 2 indicate magnetization with respect to temperature. The peak temperature of *dM/dT* corresponds to the transition temperature, indicating the martensitic transition temperature of $T_M = 338$ K (austenite phase to martensite phase). The reverse martensitic transition temperature is almost the same as T_M, with a value of 337 K, which was obtained through linear expansion in our previous study [37]. Based on the heating process of *dM/dT*, $T_R = 343$ K (martensite phase to austenite phase). From the *dM/dT* results shown in Figure 2, the martensitic transition start temperature T_{Ms}, the martensitic transition finish temperature T_{Mf}, the reverse martensitic transition start temperature T_{Rs}, and the reverse martensitic transition finish temperature T_{Rf}, was obtained as $T_{Ms} = 349$ K, $T_{Mf} = 335$ K, $T_{Rs} = 340$ K, $T_{Rf} = 353$ K. The martensitic temperature T_M as 338 K was obtained from the peak temperature of *dM/dT* during the cooling process. The reverse martensitic transition temperature T_R was obtained from the peak temperature of *dM/dT* in the heating process.
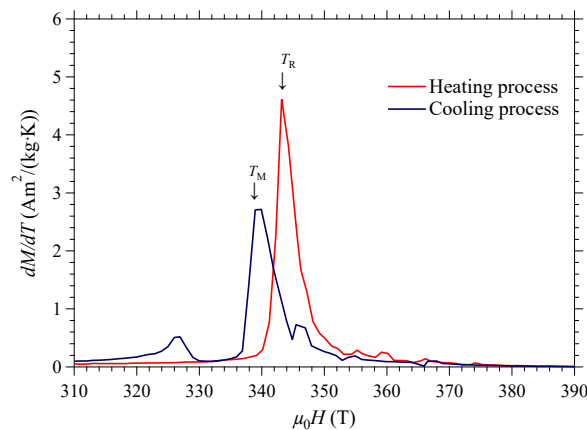

Figure 2. Differential magnetization at temperature, *dM/dT* vs. *T*, for $Ni_2MnGa_{0.88}Cu_{0.12}$ in a magnetic field of 0.1 T. T_M and T_R indicate the martensitic transition temperature and the reverse martensitic transition temperature.

In Figure 3, the magnetic field dependence of the magnetization for $Ni_2MnGa_{0.88}Cu_{0.12}$ at a constant temperature is shown. It can be observed that the martensite phase has larger magnetization than that of the austenite phase. Metamagnetic-like hysteresis was observed around 340 K. This indicates that, at the constant temperature, transition from low-magnetic field paramagnetic austenite phase to high-magnetic field ferromagnetic martensite phase

occurred. This is similar to the re-entrant transition between paramagnetic austenite phase and ferromagnetic martensite phase as shown in $Ni_2Mn_{0.7}Cu_{0.3}Ga_{0.84}Al_{0.16}$ polycrystalline alloy [19].
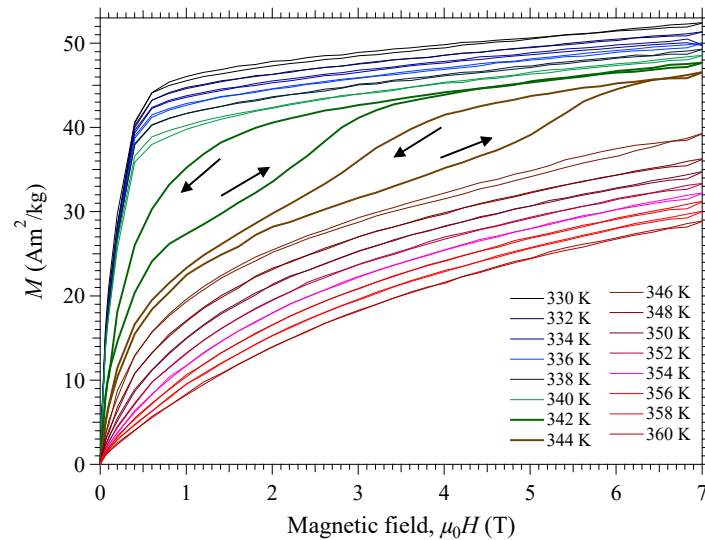

Figure 3. Magnetization process, *M* vs. *H*, for $Ni_2MnGa_{0.88}Cu_{0.12}$ from 360 to 330 K with 2 K steps. The arrows show the process of the magnetic field.

The magnetostriction was measured to investigate the relation between the structural phase transition and magnetic property.

3.2. Forced Magnetostriction

The forced magnetostriction measurements for $Ni_2MnGa_{0.88}Cu_{0.12}$ were performed from a higher temperature to a lower temperature compared to the martensite transition temperature.

Figure 4 shows the magnetic field dependence of the forced magnetostriction, $\Delta L/L$, up to 6 T. First, we measured it at 352 K, which is higher than T_M and then at a constant temperature, while gradually cooling the sample. For the y-axis ($\Delta L/L$), an offset is applied.

The magnetostriction increases when the sample is cooled from 352 K, and reaches its maximum at 1300 ppm near 343 K. Furthermore, the magnetostriction decreases when the sample is cooled. These results indicate that large magnetostriction was observed at a slightly higher temperature than the martensite transition temperature, T_M = 338 K. Furthermore, large hysteresis was observed at 345 and 343 K, which could be equivalent to the hysteresis of magnetization; in addition, re-entrant transition occurred between the paramagnetic austenite and ferromagnetic martensite phases.

As for Ni_2MnGa alloys, the rearrangement of the martensite variants is responsible for a large part of the magnetic field-induced strain. The large plastic strain observed between 341 K and 345 K indicates that this effect plays a significant and important role. In Figure 4, the magnetostriction curve at 352 K and 350 K, in the fully austenite phase, which has a temperature lower than T_{Ms} = 349 K, indicates a small hysteresis. At 348 K, the hysteresis of the magnetostriction curve is larger than that at 350 K. This indicates that the temperature was slightly lower than T_{Ms}, and thus the martensitic transition took place. At 345 K, the largest hysteresis was found. At this temperature, we expect that the austenite parent phase at low magnetic fields would change into the martensite phase. The result of thermal strain in the cooling process indicates a contraction of 1300 ppm (0.13%) with a martensitic transition around T_M [37]. The shrinkage value of the magnetostriction curve is comparable to the contraction value of the thermal strain result observed in our former study. For the isothermal magnetization process at 344 K, as shown in Figure 3, the *M-H* curve for decreasing magnetic field returns to the initial phase before the field

reaches zero, suggesting a considerable recovery of the austenite phase. Therefore, a large magnetic field-induced strain with a large hysteresis and significant austenite recovery at 345 K was observed. These results are consistent with those of $Ni_{2.15}Mn_{0.70}Cr_{0.15}Ga$ polycrystal as shown in reference [20]. From the magnetization and the magnetostriction results, the magnetic driving force is expected to be stronger than the potential barrier for the martensitic transition from the austenite phase to the martensite phase.
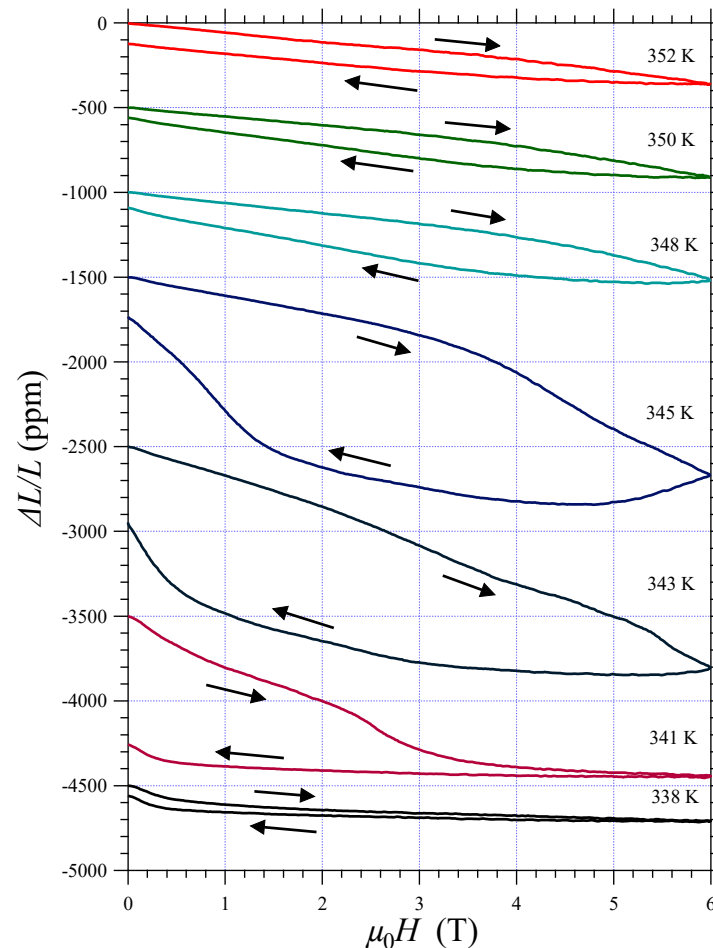

Figure 4. Magnetic field dependence of forced linear magnetostriction, $\Delta L/L$ vs. *H*, for $Ni_2MnGa_{0.88}Cu_{0.12}$. The arrows show the process of the magnetic field.

At 341 K, which is higher than $T_{Mf} = 335$ K, there are still some austenite regions in zero magnetic field. Above 4 T, the strain value was almost constant, which indicates that fully martensitic state was realized, and the variants were fully aligned in a high magnetic field. As the magnetic field-induced martensitic transition occurred at high magnetic fields, it is conceived that the recovery strain became small as it is difficult to exceed the potential barrier in low magnetic fields.

At 338 K, a nearly fully martensite state was realized even at zero magnetic field, resulting in small magnetostriction.

Figure 5 shows the magnetic field dependence of the forced magnetostriction, $\Delta L/L$, up to 9.8 T. At 345 K, the re-entrant transition is clearly identified. At 347 K, the transition shrank almost linearly with increasing magnetic fields, demonstrating hysteresis. At 345 K, the sample also shrank almost linearly with increasing magnetic fields. The shrinkage decreased beyond 8 T. When the magnetic field decreased from 9.8 T, the length of the sample remained almost the same, and below 6 T, the sample gradually lengthened. At 1.5 T, a soft kink was observed in $\Delta L/L$. The result of magnetostriction at 345 K indicates that

the magnetic-field-induced transition from the paramagnetic austenite to ferromagnetic martensite phase occurred in increasing magnetic field process.
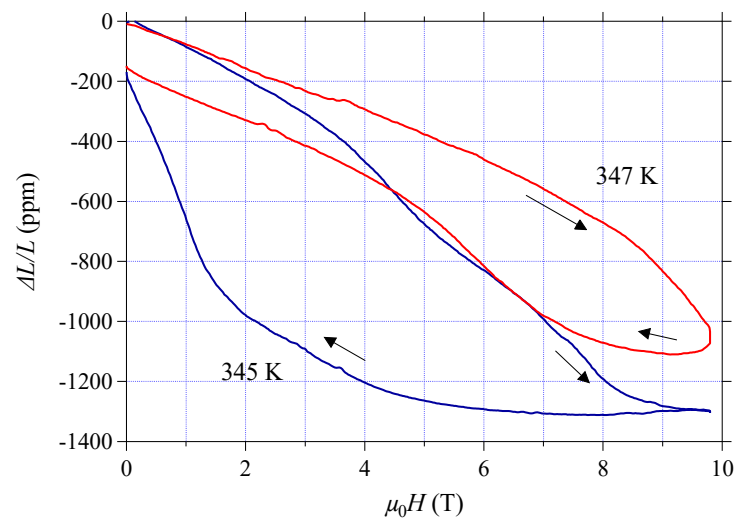

Figure 5. Magnetic field dependence of forced linear magnetostriction, $\Delta L/L$ vs. H, for $Ni_2MnGa_{0.88}Cu_{0.12}$ up to 9.8 T. The arrows show the process of the magnetic field.

In [42] and [43], regarding $Ni_2MnGa_{1-x}Cu_x$, the magnetic field was conceived to shrink because of the x dependence of Cu concentration of the unit-cell volume within the interval $0 \leq x \leq 0.25$ at room temperature. The unit-cell volume decreases with increasing x. $Ni_2MnGa_{1-x}Cu_x$ in the concentration range of $0 \leq x \leq 0.07$ crystallize in the $L2_1$ cubic structure at room temperature. The lattice parameter a_{L21} with $x = 0.02$ ($L2_1$ cubic structure) was 0.58206 nm. For $0.10 \leq x \leq 0.25$, the sample crystallizes as a $D0_{22}$-like martensite structure, as mentioned in Section 2.1. At $x = 0.12$, the unit-cell volume defined through X-ray diffraction was smaller than that of the extrapolation line at $0 \leq x \leq 0.07$ ($L2_1$ cubic structure) of the order of 0.200% (2000 ppm). The linear strain of a polycrystal is one-third of the volume strain [44]. Therefore, 670-ppm shrinkage is expected because of the austenite phase transition to the martensite phase. Moreover, in the martensite phase, the magnetic easy axis is a_{D022}, and a large shrinkage was observed with the applied magnetic field parallel to the easy axis [15]. Therefore, negative magnetostriction could be observed around T_M for this study.

3.3. Comparation with Other Ferromagnetic Magneto-Structural Alloys

Now, we compare the magneto-structural properties of $Ni_2MnGa_{0.88}Cu_{0.12}$ with other Ni_2MnGa-type ferromagnetic alloys, i.e., Ni_2MnGa [17], $Ni_{41}Co_9Mn_{31.5}Ga_{18.5}$ [31], $Ni_2Mn_{0.7}Cu_{0.3}Ga_{0.84}Al_{0.16}$ [19], and $Ni_{2.15}Mn_{0.70}Cr_{0.15}Ga$ [20] polycrystalline samples, as well as $Ni_{45}Co_5Mn_{36.7}In_{13.3}$ [7] and $Ni_{50}Mn_{30}Ga_{20}$ [5] single crystalline samples.

Table 1 provides information on the crystal structure in the martensite phase, volume change from the martensite phase to the austenite phase, and magnetostriction value of varioys Ni_2MnGa-type Heusler alloys.

Table 1. Crystal structure, volume change, and linear magnetostriction $(\Delta L/L)_{//}$ value of the Ni_2MnGa-type Heusler alloys. All alloys have the $L2_1$ cubic crystal structure in the parent austenite phase. Arrows indicate the transition direction of the magnetic and crystallographic phases.

Alloy	Crystal Structure (Martensite Phase)	Volume Change (ppm) (Paramagnetic Austenite →Ferromagnetic Martensite)	Linear Magnetostriction ($\Delta L/L$(Paramagnetic Austenite →Ferromagnetic Martensite)
Ni_2MnGa	*14M* [1]	−330 [1]	−780 [2]
$Ni_2MnGa_{0.88}Cu_{0.12}$ [3]	$D0_{22}$ + *14M*	−2000	−1300 (this study)
$Ni_{41}Co_9Mn_{31.5}Ga_{18.5}$ [4]	tetragonal	5700	1900
$Ni_{45}Co_5Mn_{36.7}In_{13.3}$ [5]	*14M*	---	30,000 (single crystal)
$Ni_2Mn_{0.7}Cu_{0.3}Ga_{0.84}Al_{0.16}$ [6]	$L1_0$	−55,000	−26,000
$Ni_{2.15}Mn_{0.70}Cr_{0.15}Ga$ [7]	$L1_0$	−30,000	−8100
$Ni_{50}Mn_{30}Ga_{20}$ [8]	*5M*	−260	−3300 (single crystal) (this study)

[1] Ref. [45] [2] Ref. [17] [3] Ref. [37] [4] Ref. [31] [5] Ref. [7] [6] Ref. [19] [7] Ref. [20] [8] Ref. [5]. The arrows indicate the transition direction of the magnetic and crystallographic phases.

Sakon et al. investigated the magnetostriction of polycrystalline sample of Ni_2MnGa [17]. The magnetostriction was measured at T = 185 K in the martensite phase, where the temperature was just below T_M = 193 K. The magnetostriction was measured parallel $(\Delta L/L)_{//}$ and perpendicular $(\Delta L/L)_\perp$ to the magnetic field. Furthermore, the obtained magnetostriction values were $(\Delta L/L)_{//}$ = −780 ppm and $(\Delta L/L)_\perp$ = 260 ppm. The volume magnetostriction $\Delta V/V$ can be obtained as follows [44–46]:

$$\Delta V/V = (\Delta L/L)_{//} + 2\,(\Delta L/L)_\perp \tag{1}$$

The obtained $\Delta V/V$ was −260 ppm. Singh et al. [45] obtained the temperature dependencies of the lattice constant and unit-cell volume based on a high-resolution synchrotron X-ray powder diffraction. The volume change from a $L2_1$ cubic structure to a monoclinic *14M* structure was −330 ppm. Volume magnetostriction $\Delta V/V$ was 80% of the volume change of the $L2_1 \rightarrow$ *14M* martensite transition.

$Ni_{41}Co_9Mn_{31.5}Ga_{18.5}$ has a T_M of 320 K and a Curie temperature, T_C of 468 K [31]. The $L2_1$ cubic ferromagnetic austenite structure and tetragonal ferrimagnetic martensite structure were obtained as magnetic and crystalline structure, respectively. Thermo-magnetic *M–T* curves indicated that at 0.5 T, a sharp magnetization jump corresponding to the thermal martensitic transition temperatures [martensite $\rightarrow$ austenite T_R = 350 K (heating process) and austenite $\rightarrow$ martensite T_M = 320 K (cooling process)] was observed at around room temperature. The T_M decreased with increasing magnetic field at the ratio of $dT_M/d(\mu_0 H)$ = −12.6 K/T. The absolute value of $dT_M/d(\mu_0 H)$ of $Ni_{41}Co_9Mn_{31.5}Ga_{18.5}$ is 10 times larger than that of $Ni_2MnGa_{0.88}Cu_{0.12}$. Below T_M, metamagnetic transitions were observed for the magnetization processes (*M-T* curves). In addition, magnetostrictions larger than 1000 ppm were observed at the temperature of 150 K $\leq T \leq$ 290 K below T_M, corresponding to a metamagnetic transition. At 290 K, the total value of magnetostriction was 1900 ppm. Assuming isotropic magnetostriction for this polycrystalline sample, the total volume change can be estimated as 5700 ppm [31]. These results indicate that below T_M, a reverse martensite transition occurred from the ferrimagnetic martensite phase to the ferromagnetic austenite phase with the increasing magnetic field. The experimental and theoretical results show that the total energy of the ferromagnetic state is close to that of the ferrimagnetic martensite state, and the magnetic-field-induced ferromagnetic austenite phase is unstable in the ratio of the tetragonality (*c/a*) for 1.0 $\leq c/a \leq$ 1.1. Therefore, metamagnetic transitions and large magnetostrictions were observed in the magnetic field.

A single crystal of $Ni_{45}Co_5Mn_{36.7}In_{13.3}$ indicates a large MFIS of 30,000 ppm (3.0%) at 298 K when a compressive pre-strain of approximately 3% was applied in the direction

plotted with a filled circle in the stereographic triangle, as shown in Figure 4 of Ref. [7]. The magnetic field was applied parallel to the compressive axis of the sample. The T_{M} was 290 K and T_{C} was 382 K. Below this T_{M}, the *M-T* curve indicated a clear metamagnetic transition behavior. The T_{M} decreased with increasing magnetic field at the ratio of $dT_{\mathrm{M}}/d(m_0H) = -7$ K/T, and an $L2_1$ cubic structure was achieved in austenite phase, and a monoclinic *14 M* layered structure was achieved in the martensite phase. Below T_{M}, the MFIS was observed to occur during the metamagnetic transition from the ferrimagnetic martensite phase to ferromagnetic austenite phase. The strain from the $L2_1$ cubic structure to monoclinic *14 M* layered structure is significant, exceeding a few percent. For example, Sozinov et al. experimentally studied the MFIS of a single-variant sample of an orthorhombic seven-layered phase in the $Ni_{48.8}Mn_{29.7}Ga_{21.5}$ single crystalline alloy at 300 K, measuring it perpendicular to the magnetic field applied along the [100] direction [3]. They observed a giant MFIS of approximately 95,000 ppm (9.5%) at an ambient temperature in a magnetic field of less than 1 T in the Ni_2MnGa orthorhombic seven-layered (*7M* structure, which corresponds to *14M* structure) martensite phase.

On the contrary, the crystal structure of $Ni_{41}Co_9Mn_{31.5}Ga_{18.5}$ is not a monoclinic *14 M* structure but a tetragonal structure, and the volume change due to the martensitic transition is 5700 ppm. Therefore, a moderate magnitude magnetostriction was observed.

In the case of $Ni_2MnGa_{0.88}Cu_{0.12}$, the value of the magnetostriction (1300 ppm) is the same order as that of $Ni_{41}Co_9Mn_{31.5}Ga_{18.5}$ (1900 ppm). The tetragonal phase of the $D0_{22}$-like crystal structure coexists with the monoclinic phase of the monoclinic *14M* structure (space group: *P2/m*) in the martensite phase at room temperature. The volume change from the $L2_1$ cubic structure to monoclinic *14M* structure was -330 ppm for Ni_2MnGa [45]. Therefore, -1300 ppm magnetostriction, which is smaller than that of $Ni_{41}Co_9Mn_{31.5}Ga_{18.5}$, the crystal structure of which is a tetragonal martensite, is suitable for the $Ni_2MnGa_{0.88}Cu_{0.12}$ polycrystalline alloy.

As mentioned earlier, for $Ni_2Mn_{0.7}Cu_{0.3}Ga_{0.84}Al_{0.16}$, $T_{\mathrm{M}} = 293$ K and the martensitic and ferromagnetic transitions occur at the same temperature, as confirmed by the magnetization and magnetostriction measurements [19]. In addition, the results of X-ray powder diffraction measurement indicated that the crystal structure was $L2_1$ cubic austenite at 312 K. Moreover, at 298 K, which is slightly higher than $T_{\mathrm{M}} = 293$ K, the austenitic $L2_1$ cubic structure and martensitic $L1_0$ non-modulated tetragonal structure were observed to coexist. Finally, below 257 K, the $L1_0$ structure was achieved.

The unit-cell volume of $Ni_2Mn_{0.7}Cu_{0.3}Ga_{0.84}Al_{0.16}$ calculated by the lattice parameters showed the volume difference between the austenite $L2_1$ phases and martensite $L1_0$ phase as approximately $-55,000$ ppm (-5.5%). Therefore, a giant magnetostriction was expected around $-18,000$ ppm (-1.8%) for the polycrystalline sample. However, the experimental results showed magnetostriction of $\Delta L/L = -26,000$ ppm (-2.6%.), which is larger than the expected value. Therefore, the effect of the alignment of the variant of martensite must be considered. The magnetostriction is irreversible during the experimental temperatures of $297.4\,\mathrm{K} \leq T \leq 304$ K. Partial recovery was observed only at 305 K.

In the case of $Ni_2MnGa_{0.88}Cu_{0.12}$, the value of the magnetostriction was one-tenth that of $Ni_2Mn_{0.7}Cu_{0.3}Ga_{0.84}Al_{0.16}$. However, an 85% recovery strain was observed at 345 K. The existence of recovery strain at atmospheric pressure is advantageous for the alloy's application in sensors and actuators.

Mendonça et al. [20] performed the magnetostriction measurements on the $Ni_{2.15}Mn_{0.70}Cr_{0.15}Ga$ polycrystalline alloy with $T_{\mathrm{M}} = 299$ K. In addition, the martensitic and ferromagnetic transitions occurred at the same temperature, as confirmed by the magnetization and magnetostriction measurements. The resulting crystal structure in the parent austenite phase was the $L2_1$ cubic structure. The martensite phase is an $L1_0$ non-modulated tetragonal structure. The unit-cell volume of $Ni_2Mn_{0.7}Cu_{0.3}Ga_{0.84}Al_{0.16}$ calculated from the lattice parameters showed that the volume difference between the austenite $L2_1$ phases and martensite $L1_0$ phase is approximately $-30,000$ ppm (-3.0%). The magnetostriction results indicated a reversible strain around -8100 ppm (-0.81%) under 0–9 T, which is slightly lesser

than one-third the volume difference ($-10,000$ ppm, -1.0%). Mendonça et al. [20] overcame the weak point of large hysteresis in the magnetostriction of $Ni_2Mn_{0.7}Cu_{0.3}Ga_{0.84}Al_{0.16}$. The characteristic of a magneto-structural transformation at room temperature with low hysteresis is advantageous for the alloy's application in functional magnetic materials. In this experimental study, the value of the magnetostriction of $Ni_2MnGa_{0.88}Cu_{0.12}$ is one-sixth of that of $Ni_{2.15}Mn_{0.70}Cr_{0.15}Ga$. However, it is advantageous for its industrial application and possesses smaller magnetostriction than that of $Ni_{2.15}Mn_{0.70}Cr_{0.15}Ga$.

As a reference sample, we measured the magnetostriction of the Ni_2MnGa-type ($Ni_{50}Mn_{30}Ga_{20}$) alloy manufactured by Adaptamat Co., Ltd. [4,5], which is shown in Figure 6. This alloy causes martensite phase transition at T_M = 315 K. Magnetostriction of $Ni_{50}Mn_{30}Ga_{20}$ was measured parallel to the magnetic field, which was parallel to the c-axis. Magnetostriction of -3300 ppm was observed at an atmospheric pressure and 298 K. Almost 100% recovery strain was observed. The value of the magnetostriction of $Ni_2MnGa_{0.88}Cu_{0.12}$ was one-third that of $Ni_{50}Mn_{30}Ga_{20}$. However, the value of the magnetostriction of $Ni_2MnGa_{0.88}Cu_{0.12}$ is larger than that of Terfenol-D (800 ppm), which is renowned as the most commonly used magnetostrictive alloy [47,48].
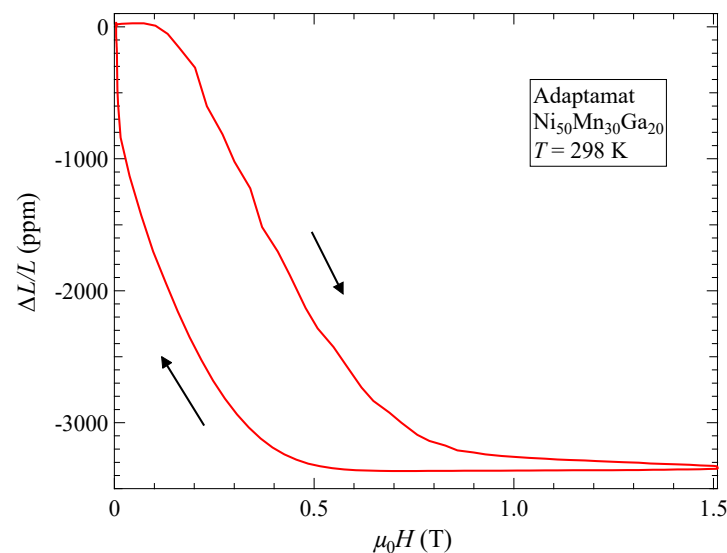

Figure 6. Magnetic field dependence of forced linear magnetostriction, $\Delta L/L$ vs. H, for $Ni_{50}Mn_{30}Ga_{20}$. The arrows show the process of the magnetic field.

As mentioned above, a shrinkage of -3300 ppm was observed at 298 K in the martensite phase. This result is comparable to magnetostriction of Ni_2MnGa single crystal at atmospheric pressure (unstressed crystal) measured by Ullakko et al. [1]. The martensitic transition temperature, T_M, was 275 K. In the martensite phase at 265 K, a magnetostriction value of the [001] axis (c-axis in a martensite phase) strain in response to magnetic field applied along c-axis was—1000 ppm in an applied magnetic field of 1 T. Ullakko et al. mentioned that the strain occurs fully within the martensitic phase and is due to the motion of twin boundaries. The magnetostriction is only a small fraction of the lattice constant change ($\Delta c/c$ = 6.56% = 65,600 ppm). They also mentioned that this small strain is caused by the strain accommodation through different twin variant orientations. In the martensite phase, applying the magnetic field to the single variant material causes the other twin variants to appear and grow [3,4]. When magnetic field strength increases the boundaries between twins move, and the preferentially oriented twin variants grow at the expense of the other twin variants. It is interesting that the magnetostriction of $Ni_{50}Mn_{30}Ga_{20}$ (this study) and Ni_2MnGa [1] was almost fully reversible. Currently, we cannot explain why the recovery of strain occurred in the martensite phase. It is conceived that the rearrangements of the twin variants would occur when increasing a magnetic field, and afterwards, during the decreasing magnetic field process, elastic recovery may act and come back to the origi-

nal state. However, the exact reason for this recovery is currently not clear. Recently, Wu et al. simulated the ferromagnetic domain structure and martensite variant microstructure of Ni_2MnGa-type shape-memory alloy [12]. They found -0.28% (-2800 ppm) magnetic field induced strain and also found 100% recovery strain at 285 K below $T_M = 300$ K. This value is comparable with our result of $Ni_{50}Mn_{30}Ga_{20}$ alloy. We retrieve this model helps explanation of the recovery strain.

4. Conclusions

In this study, magnetostriction measurements were performed on the ferromagnetic Heusler alloy $Ni_2MnGa_{0.88}Cu_{0.12}$. One characteristic of this alloy is that its martensitic and ferromagnetic transitions are caused at the same temperature. In the austenite and martensite phases, the alloy crystallizes with $L2_1$ and $D0_{22}$-like crystal structures, respectively. Metamagnetic transition was observed in the magnetic field of $\mu_0H = 4$ T at 344 K. This result showed that the occurrence of phase transition was induced by the magnetic field under constant temperature. Forced magnetostriction measurements ($\Delta L/L$) were performed under constant temperature and at an atmospheric pressure of $P = 0.1$ MPa. Magnetostriction up to 1300 ppm was observed around the T_M. The magnetization and magnetostriction measurement results showed that the magnetic-field-induced strain from the paramagnetic austenite phase to ferromagnetic martensite phase occurred. In the case of $Ni_2MnGa_{0.88}Cu_{0.12}$, the value of the magnetostriction was one-tenth that of $Ni_2Mn_{0.7}Cu_{0.3}Ga_{0.84}Al_{0.16}$, which has a tetragonal $L1_0$ martensite structure. However, 85% recovery strain was observed at 345 K. The value of the magnetostriction of $Ni_2MnGa_{0.88}Cu_{0.12}$ was one-sixth that of $Ni_{2.15}Mn_{0.70}Cr_{0.15}Ga$, which has low hysteresis and reversible strain in magnetic fields. The existence of a recovery strain at atmospheric pressure is advantageous to the alloy's application to sensors and actuators.

For reference, we measured the magnetostriction of the Ni_2MnGa-type ($Ni_{50}Mn_{30}Ga_{20}$) alloy made in Adaptamat Co., Ltd. The magnetostriction of -3300 ppm was observed at 298 K, and almost 100% recovery strain was observed. The value of the magnetostriction of $Ni_2MnGa_{0.88}Cu_{0.12}$ was one-third that of $Ni_{50}Mn_{30}Ga_{20}$. However, the value of the magnetostriction of $Ni_2MnGa_{0.88}Cu_{0.12}$ is larger than that of Terfenol-D (800 ppm).

Author Contributions: Y.A. and T.K. prepared the samples; T.S., H.N., Y.N., M.H. and T.K. conceived and designed the experiments; K.M., T.K., H.N., Y.N., M.H. and T.S. performed the experiments; K.M. and T.S. analyzed the data; T.S., K.M., T.K., Y.N., M.H., H.N. and Y.A. wrote the paper. All authors have read and agreed to the published version of the manuscript.

References

1. Ullakko, K.; Huang, J.K.; Kantner, C.; O'Handley, R.C.; Kokorin, V.V. Large magnetic-field-induced strains in Ni_2MnGa single crystals. *Appl. Phys. Lett.* **1996**, *69*, 1966–1968. [CrossRef]
2. Ullakko, K.; Huang, J.K.; Kokorin, V.V.; O'Handley, R.C. Magnetically controlled shape memory effect in Ni_2MnGa intermetallics. *Scr. Mater.* **1997**, *36*, 1133–1138. [CrossRef]
3. Sozinov, A.; Likhachev, A.A.; Lanska, N.; Ullakko, K. Giant magnetic-field-induced strain in NiMnGa seven-layered martensitic phase. *Appl. Phys. Lett.* **2002**, *80*, 1746–1748. [CrossRef]
4. Tellinen, J.; Suorsa, I.; Jääskeläinen, A.; Aaltio, I.; Ullakko, K. Basic properties of magnetic shape memory actuators. In Proceedings of the 8th International Conference ACTUATOR, Bremen, Germany, 10–12 June 2002; pp. 566–569.

5. Ge, Y.; Söderberg, O.; Lanska, N.; Sozinov, A.; Ullakko, K.; Lindroos, V.K. Crystal structure of three Ni-Mn-Ga alloys in powder and bulk materials. *J. Phys. IV* **2003**, *112*, 921–924. [CrossRef]

6. Chernenko, V.A.; L'vov, V.A. Magnetoelastic nature of ferromagnetic shape memory effect. *Mater. Sci. Forum* **2008**, *583*, 1–20. [CrossRef]

7. Kainuma, R.; Imano, Y.; Ito, W.; Sutou, Y.; Morito, H.; Okamoto, S.; Kitakami, O.; Oikawa, K.; Fujita, A.; Kanomata, T.; et al. Magnetic-field-induced shape recovery by reverse phase transformation. *Nature* **2006**, *439*, 957–960. [CrossRef]

8. Sakon, T.; Sasaki, K.; Numakura, D.; Abe, M.; Nojiri, H.; Adachi, Y.; Kanomata, T. Magnetic field-induced transition in co-doped $Ni_{41}Co_9Mn_{31.5}Ga_{18.5}$ heusler alloy. *Mater. Trans.* **2013**, *54*, 9–13. [CrossRef]

9. Karaca, H.E.; Karaman, I.; Basaran, B.; Ren, Y.; Chumlyakov, Y.I.; Maier, H.J. Magnetic field-induced phase transformation in NiMnCoIn magnetic shape-memory alloys—A new actuation mechanism with large work output. *Adv. Funct. Mater.* **2009**, *19*, 983–998. [CrossRef]

10. Kainuma, R.; Oikawa, K.; Ito, W.; Sutou, Y.; Kanomata, T.; Ishida, K. Metamagnetic shape memory effect in NiMn-based Heusler-type alloys. *J. Mater. Chem.* **2008**, *18*, 1837. [CrossRef]

11. O'Handley, R.C.; Murray, S.J.; Marioni, M.; Nembach, H.; Allen, S.M. Phenomenology of giant magnetic-field-induced strain in ferromagnetic shape memory materials. *J. Appl. Phys.* **2000**, *87*, 4712–4717. [CrossRef]

12. Wu, P.; Liang, Y. Enhanced reversible magnetic-field-induced strain in Ni-Mn-Ga Alloy. *Metals* **2021**, *11*, 2017. [CrossRef]

13. Kumar, A.S.; Seshubai, V. 0.7% magnetic field induced strain in polycrystalline $Ni_{50}Mn_{29}Ga_{21}$ ferromagnetic shape memory alloy. *Int. J. Innov. Res. Sci. Eng. Technol.* **2013**, *2*, 4226–4232.

14. Mennerich, C.; Wendler, F.; Jainta, M.; Nestler, B. Rearrangement of martensitic variants in Ni_2MnGa studied with the phase-field method. *Eur. Phys. J. B* **2013**, *86*, 171. [CrossRef]

15. Okamoto, N.; Fukuda, T.; Kakeshita, T.; Takeuchi, T.; Kishino, K. Rearrangement of variants in Ni_2MnGa under magnetic field. *Sci. Technol. Adv. Mater.* **2004**, *5*, 29–34. [CrossRef]

16. Sakon, T.; Fujimoto, N.; Kanomata, T.; Adachi, Y. Magnetostriction of $Ni_2Mn_{1-x}Cr_xGa$ heusler alloys. *Metals* **2017**, *7*, 410. [CrossRef]

17. Sakon, T.; Yamasaki, Y.; Kodama, H.; Kanomata, T.; Nojiri, H.; Adachi, Y. The characteristic properties of magnetostriction and magneto-volume effects of Ni_2MnGa-type ferromagnetic heusler alloys. *Materials* **2019**, *12*, 3655. [CrossRef] [PubMed]

18. Sakon, T.; Adach, Y.; Kanomata, T. Magneto-structural properties of Ni_2MnGa ferromagnetic shape memory alloy in magnetic fields. *Metals* **2013**, *3*, 202–224. [CrossRef]

19. Mendonça, A.A.; Jurado, J.F.; Stuard, S.J.; Silva, L.E.L.; Eslava, G.G.; Cohen, L.F.; Ghivelder, L.; Gomes, A.M. Giant magnetic-field-induced strain in Ni_2MnGa-based polycrystal. *J. Alloys Compd.* **2018**, *738*, 509–514. [CrossRef]

20. Mendonça, A.A.; Ghivelder, L.; Bernardo, P.L.; Cohen, L.F.; Gomes, A.M. Low hysteretic magnetostructural transformation in Cr-doped Ni-Mn-Ga Heusler alloy. *J. Alloys Compd.* **2023**, *938*, 168444. [CrossRef]

21. Sofronie, M.; Tolea, F.; Tolea, M.; Popescu, B.; Valeanu, M. Magnetic and magnetostrictive properties of the ternary $Fe_{67.5}Pd_{30.5}Ga_2$ ferromagnetic shape memory ribbons. *J. Phys. Chem. Sol.* **2020**, *142*, 109446. [CrossRef]

22. Mahfouzi, M.; Carman, G.P.; Kioussis, N. Magnetoelastic and magnetostrictive properties of Co2XAl Heusler compounds. *Phys. Rev. B* **2020**, *102*, 094401. [CrossRef]

23. Sofronie, M.; Tolea, M.; Popescu, B.; Enculescu, M.; Tolea, F. Magnetic and Magnetostrictive Properties of $Ni_{50}Mn_{20}Ga_{27}Cu_3$ Rapidly Quenched Ribbons. *Materials* **2021**, *14*, 5126. [CrossRef]

24. Liu, K.; Ma, S.; Zhang, Y.; Zeng, H.; Yu, G.; Luo, X.; Chena, C.; Rehman, S.U.; Hu, Y.; Zhong, Z. Magnetic-field-driven reverse martensitic transformation with multiple magneto-responsive effects by manipulating magnetic ordering in Fe-doped Co-V-Ga Heusler alloys. *J. Mater. Sci. Technol.* **2020**, *58*, 145–154. [CrossRef]

25. Kaštil, J.; Kamarád, J.; Míšek, J.; Isnard, O.; Amara, M.; Arnold, Z. Magnetostriction and extraordinary exchange spring and exchange bias effects in $Ni_{48}Mn_{39}Sn_{13}$ Heusler alloy. *Intermetallics* **2021**, *132*, 109137. [CrossRef]

26. Huang, Y.; Qian, J.; Dong, D.; Shi, Y.; Du, Y.; Tang, S. Magnetostriction in <0kl>-oriented composites with CoMnSi microspheres. *J. Magn. Magn. Mater.* **2022**, *543*, 168621.

27. Liua, J.; Gonga, Y.; Zhang, F.; Youa, Y.; Xu, G.; Miao, X.; Xu, F. Large, low-field and reversible magnetostrictive effect in MnCoSi-based metamagnet at room temperature. *J. Mater. Sci. Technol.* **2021**, *76*, 104–110. [CrossRef]

28. Minorowicz, B.; Milecki, A. Design and Control of Magnetic Shape Memory Alloy Actuators. *Materials* **2022**, *15*, 4400. [CrossRef]

29. Kurita, H.; Keino, T.; Senzaki, T.; Narita, F. Direct and inverse magnetostrictive properties of Fe–Co–V alloy particle-dispersed polyurethane matrix soft composite sheets. *Sens. Actuators A Phys.* **2022**, *337*, 113427. [CrossRef]

30. Sadeghzadeh, A.; Asua, E.; Feuchtwanger, J.; Etxebarria, V.; García-Arribas, A. Ferromagnetic shape memory alloy actuator enabled for nanometric position control using hysteresis compensation. *Sens. Actuators A Phys.* **2012**, *182*, 122–129. [CrossRef]

31. Kihara, T.; Roy, T.; Xu, X.; Miyake, A.; Tsujikawa, M.; Mitamura, H.; Tokunaga, M.; Adachi, Y.; Eto, T.; Kanomata, T. Observation of inverse magnetocaloric effect in magnetic-field-induced austenite phase of Heusler alloys Ni50−xCoxMn31.5Ga18.5 (x = 9 and 9.7). *Phys. Rev. Mater.* **2021**, *5*, 034416. [CrossRef]

32. Hennel, M.; Galdun, L.; Džubinská, A.; Reiffers, M.; Varga, R. High efficiency direct magnetocaloric effect in Heusler Ni_2MnGa microwire at low magnetic fields. *J. Alloys Compd.* **2023**, *960*, 170621. [CrossRef]

33. Brock, J.; Khan, M. Large refrigeration capacities near room temperature in $Ni_2Mn_{1-x}Cr_xIn$. *J. Magn. Magn. Mater.* **2017**, *425*, 1–5. [CrossRef]

34. Zheng, T.; Liu, K.; Chen, H.; Wang, C. Large magnetocaloric and magnetoresistance effects during martensitic transformation in Heusler-type $Ni_{44}Co_6Mn_{37}In_{13}$ alloy. *J. Magn. Magn. Mater.* **2022**, *563*, 170034. [CrossRef]
35. Salazar-Mejía, C.; Devi, P.; Singh, S.; Felser, C.; Wosnitza, J. Influence of Cr substitution on the reversibility of the magnetocaloric effect in Ni-Cr-Mn-In Heusler alloys. *Phys. Rev. Mater.* **2021**, *5*, 104406. [CrossRef]
36. Kitanovski, A. Energy applications of magnetocaloric materials. *Adv. Energy Mater.* **2020**, *10*, 1903741. [CrossRef]
37. Sakon, T.; Nagashio, H.; Sasaki, K.; Susuga, S.; Numakura, D.; Abe, M.; Endo, K.; Nojiri, H.; Kanomata, T. Thermal expansion and magnetization studies of the novel ferromagnetic shape memory alloy $N_2MnGa_{0.88}Cu_{0.12}$ in a magnetic field. *Phys. Scr.* **2011**, *84*, 045603. [CrossRef]
38. Khovailo, V.V.; Takagi, T.; Tani, J.; Levitin, R.Z.; Cherechukin, A.A.; Matsumoto, M.; Note, R. Magnetic properties of Ni2.18Mn0.82Ga heusler alloys with a coupled magnetostructural transition. *Phys. Rev. B* **2002**, *65*, 092410. [CrossRef]
39. Filippov, D.A.; Khovailo, V.V.; Koledov, V.V.; Krasnoperov, E.P.; Levitin, R.Z.; Shavrov, V.G.; Takagi, T. The magnetic field influence on magnetostructural phase transition in $Ni_{2.19}Mn_{0.81}Ga$. *J. Magn. Magn. Mater.* **2003**, *258*, 507–509. [CrossRef]
40. Khovailo, V.V.; Novosad, V.; Takagi, T.; Filippov, D.A.; Levitin, R.Z.; Vasil'ev, A.N. Magnetic properties and magnetostructural phase transitions in shape memory alloys. *Phys. Rev. B* **2004**, *70*, 174413. [CrossRef]
41. Gonzàlez-Comas, A.; Obradó, E.; Mañosa, L.; Planes, A.; Chernenko, V.A.; Hattink, B.J.; Labarta, A. Premartensitic and martensitic phase transitions in ferromagnetic Ni_2MnGa. *Phys. Rev. B* **1999**, *60*, 7085–7090. [CrossRef]
42. Endo, K.; Kanomata, T.; Kimura, A.; Kataoka, M.; Nishihara, H.; Umetsu, R.Y.; Obara, K.; Shishido, T.; Nagasako, M.; Kainuma, R.; et al. Magnetic phase diagram of the ferromagnetic shape memory alloys $Ni_2MnGa_{1-x}Cu_x$. *Mater. Sci. Forum* **2011**, *684*, 165–176. [CrossRef]
43. Kanomata, T.; Endo, K.; Kudo, N.; Umetsu, R.Y.; Nishihara, H.; Kataoka, M.; Nagasako, M.; Kainuma, R.; Ziebeck, K.R.A. Magnetic moment of Cu-modified Ni_2MnGa magnetic shape memory alloys. *Metals* **2013**, *3*, 114–122. [CrossRef]
44. Kittel, C. *Introduction of Solid State Physics*, 8th ed.; John Wiley & Sons Inc.: Hoboken, NJ, USA, 2004; p. 75.
45. Singh, S.; Bednarcik, J.; Barman, S.R.; Felser, C.; Pandey, D. Premartensite to martensite transition and its implications for the origin of modulation in Ni_2MnGa ferromagnetic shape memory alloy. *Phys. Rev. B* **2015**, *92*, 054112. [CrossRef]
46. Nizhankovskii, V.I. Classical magnetostriction of nickel in high magnetic field. *Eur. Phys. J. B* **2006**, *53*, 1–4. [CrossRef]
47. Wang, Z.; Liu, J.; Jiang, C.; Xu, H. The stress dependence of magnetostriction hysteresis in TbDyFe [110] oriented crystal. *J. Appl. Phys.* **2011**, *109*, 123923. [CrossRef]
48. Sakon, T.; Matsumoto, T.; Komori, T. Rotation angle sensing system using magnetostrictive alloy Terfenol-D and permanent magnet. *Sens. Actuators A* **2021**, *321*, 112588. [CrossRef]